Determination of the effective Young's modulus of vertically aligned carbon nanotube arrays: a simple nanotube-based varactor

Cite as:
Olofsson, N., Ek-Weis, J., Eriksson, A., Idda, T., & Campbell, E. E. B. (2009). Determination of the effective Young's modulus of vertically aligned carbon nanotube arrays: a simple nanotube-based varactor. *Nanotechnology*, 20(38), [385710].

Manuscript received: 01/07/2009; Article published: 28/08/2009

Determination of the effective Young's modulus of vertically aligned carbon nanotube arrays: a simple nanotube-based varactor**

Niklas Olofsson,[1] Johan Ek-Weis,[2] Anders Eriksson,[1] Tonio Idda[3] and Eleanor E B Campbell[2,4]

[1]Department of Physics, Göteborg University, SE-41296 Göteborg, Sweden.

[2]EaStCHEM, School of Chemistry, Joseph Black Building, University of Edinburgh, West Mains Road, Edinburgh, EH9 3JJ, UK.

[3]LAAS-CNRS, 7 Avenue du Colonel Roche, 31077 Toulouse Cedex, France.

[4]Department of Physics, Konkuk University, Seoul 143-701, Korea.

[*]Corresponding author; e-mail: eleanor.campbell@ed.ac.uk

[**]Financial support from the EU NANORF STREP programme, The Knut and Alice Wallenberg Foundation, Vetenskapsrådet, EastChem and the Gothenburg University Nanoparticles Platform is gratefully acknowledged. This paper reflects the views of the authors and not necessarily those of the EC. The community is not liable for any use that may be made of the information contained herein.

Abstract

The electromechanical properties of arrays of vertically aligned multiwalled carbon nanotubes were studied in a parallel plate capacitor geometry. The electrostatic actuation was visualized using both optical microscopy and scanning electron microscopy and highly reproducible behaviour was achieved for actuation voltages below the pull-in voltage. The walls of vertically aligned carbon nanotubes behave as solid cohesive units. The effective Young's modulus for the carbon nanotube arrays was determined by comparing the actuation results with the results of electrostatic simulations and was found to be exceptionally low, on the order of 1-10 MPa. The capacitance change and Q-factor were determined by measuring the frequency dependence of the radio-frequency transmission. Capacitance changes of over 20% and Q-factors in the range 100 - 10 were achieved for a frequency range of 0.2 – 1.5 GHz.

1. Introduction

Carbon nanotubes have exceptional mechanical, electrical and thermal properties that make them interesting materials for a wide range of applications [1]. The low mass combined with high strength, high conductivity and resistance to radiation and temperature is advantageous for the fabrication of composite materials or for micro- and nanoscale electronics and actuation applications. In addition to the interesting properties of individual nanotubes or nanotubes embedded in composites, there is a third class of nanotube material with very intriguing properties. It is possible to grow vertically aligned carbon nanotube arrays that are being investigated e.g. as a means of fabricating vertical interconnects on microchips,[2] as field emission electron sources [3] or as MEMS thermal switches [4]. Nanotubes from such arrays have also been "drawn out" to produce large area films that are considered to be aerogels and are being studied as promising actuator materials [5]. It is possible to grow such vertically aligned carbon nanotube arrays in a variety of geometries, determined by the catalyst pattern prepared by photo- or e-beam lithography, and the height of the arrays (from a few microns to mm) can be determined by the growth time and conditions [6]. However, little is known concerning the mechanical and actuation properties of directly grown vertically- aligned carbon nanotube structures. A number of studies have shown that nanotube arrays can be easily compressed with the nanotubes collectively forming zig-zag buckles that can unfold to their original length when the load is removed [7]. On the basis of these studies it was suggested that the nanotube films or arrays could be suitable as energy-absorbing coatings. In this paper we study the mechanical properties of such arrays by fabricating a simple parallel- plate capacitor. We show that walls of vertically aligned carbon nanotubes can be easily and reproducibly actuated by applying a relatively low voltage and that the walls behave as a single entity, retaining the original pattern. The wall separation can thus be changed by applying a voltage, forming a simple varactor. The effective Young's modulus of the structures is shown to be exceptionally low, on the order of 5 MPa, which is even lower than that of rubber. This can be related to the very low density and "spaghetti-like" quasi- alignment of the nanotubes in the walls. Although the demonstrated device is not

competitive with current varactors in terms of tuning range, the relatively low actuation voltage and the inherent properties of the nanotube material makes this a promising route for the development of micro- and nano-electromechanical elements. The present studies, showing that the behaviour can be very well modelled using standard MEMS software, should provide the impetus for the design of electromechanical elements taking advantage of the exceptional mechanical and electrical properties of the nanotube arrays.

2. Fabrication and Measurement Setup

The vertically aligned multiwalled carbon nanotube arrays were grown on 200 nm thick Mo electrodes with a 10nm thick Ti adhesion layer prepared by electron-beam lithography. The catalyst layer deposited on top of the Mo electrodes consisted of 5 nm Al_2O_3 followed by 1 nm Fe. The nanotubes were grown by thermal chemical vapor deposition in a quartz furnace at 700 ^oC and atmospheric pressure using a gas mixture of 5.0 sccm acetylene, 500 sccm hydrogen and 500 sccm argon for 150 seconds [8]. The catalyst areas had a U-shape with a length of 200 μm, array width of 4 μm (unless otherwise stated) and a lateral separation of 10 μm. The resulting nanotubes were multiwalled with diameters in the range 5-10 nm and typically 5 walls with a length of 135 ± 5 μm. The density of the nanotube arrays was determined by measuring the geometry of the grown structures in SEM and determining the weight of the nanotubes by weighing the substrate with the nanotubes and after removing the nanotubes by pyrolysis. The arrays were found to have a very low density of ca. 10 kg m^{-3}, corresponding to 10^{10} nanotubes cm^{-2}.

To enable high-frequency electrical measurements of the device capacitance, a wafer of p-type high resistive Si (resistivity > 9000 Ωcm) with 600 nm polysilicon followed by a 400 nm SiO_2 layer [9] was used. The layout for the varactor device is shown in Fig. 1(a). The U-shape was chosen to provide some mechanical stability for the thin nanotube walls to improve the vertical alignment of the structures. It is expected that alignment can be improved by increasing the density of the nanotubes in the arrays, at the expense of a somewhat higher actuation voltage for the device. An SEM image of a directly-grown varactor is shown in Fig. 1(b). Each varactor device consisted of two opposing T-shaped electrodes (on which the nanotubes were grown), both connected to metal pads to enable electrical connection.

In order to optimize the variable capacitance measurements, the electrode area was minimized and surrounded by shield electrodes [10]. The Mo electrodes were deposited by sputtering. This was found to give an order of magnitude lower resistivity than electron-beam evaporated Mo thin films of the same thickness. The value of the capacitance for a given actuation voltage was found by measuring the S-parameters in the range from 200 MHz to 1.5 GHz by using a probe station connected to an Agilent E5071B network analyzer [11]. The shield electrodes were connected to ground during the measurements to form a coplanar ground- signal-ground (GSG) to fit GSG probes. The signal line width was narrowed (Fig. 1) to give less parasitic capacitance contribution to S_{21} to improve the sensitivity. Reference measurements were carried out with a THRU sample

(with a short circuit between the electrodes) and with an OPEN sample (without carbon nanotubes) in order to extract the values for the resistances and capacitances of the electrodes, inherent to their material and geometry. The network analyzer was calibrated using a "SOLT" calibration.

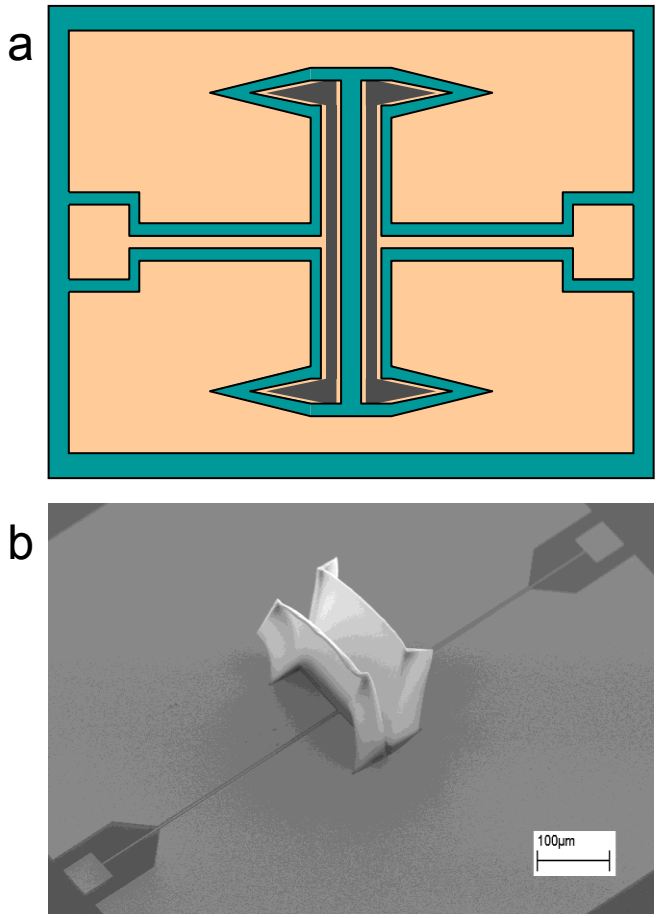

Figure 1. (a) Layout of the vractor substrate. Electrodes are shown in orange (light shading), insulating areas in blue (dark shading). The position of the U-shaped CNT arrays are shown in black, they are separated by 10 µm. (b) SEM picture of a directly grown varactor device. The CNT arrays have a width of 4 µm and a height of 135 µm.

The varactor device was simulated with the 3D full-wave simulator HFSS and the S- parameter responses were extracted to evaluate the device parasitics and were compared to the actual experimental devices. The nanotube walls were simulated as a conductive material with a density of 10 kg m^{-3}. Electrostatic simulations of the devices were conducted in the COMSOL multiphysics tool and electrodynamical simulations were conducted using COVENTOR software. The Young's modulus of the nanotube arrays was treated as a fitting parameter.

3. Determination of Young's modulus of aligned multiwalled carbon nanotube arrays

Figure 2 shows snapshots obtained when actuating varactor devices in an optical microscope (Fig. 2(a) – (d)) and in a scanning electron microscope (SEM) (Fig. 2 (e) – (h)). For the optical microscope measurement, the microscope was focused on the top of the array. In both cases, one can clearly see a decrease in the separation between the tops of the walls as the voltage between the nanotube walls is increased. The SEM pictures provide a better overall picture of the actuation. Note that the brightness of the walls changes as the applied voltage changes. The lower wall, which has a positive potential applied to it, appears darker since it is more difficult for the secondary electrons to escape [12].

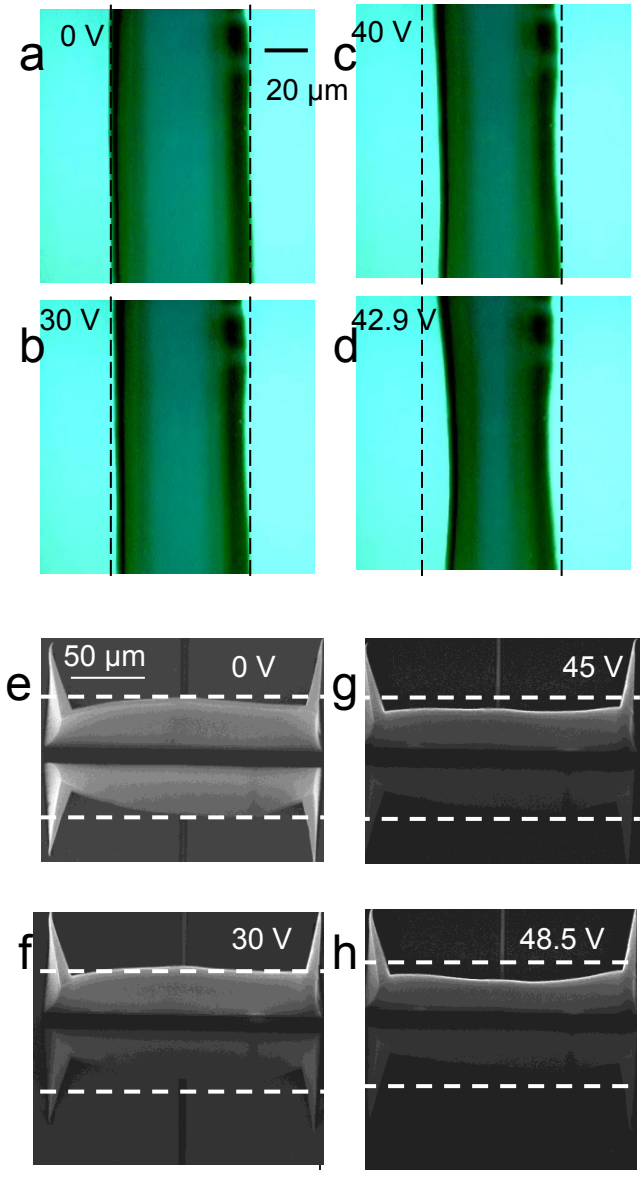

Figure 2. (a)-(d) Optical microscope images focused on top of the varactor walls, imaged for different applied voltages (a) 0V, (b) 30 V, (c) 40 V and 9d) 42.9 V. (e)-(h) SEM images looking down on a different varactor

device taken at different applied voltages (e) 0 V, (f) 30 V, (g) 45 V, (h) 48.5 V. The lower image becomes darker as the (positive) voltage is increased on the lower electrode due to the increasing difficulty for the secondary electrons to escape.

The voltages required for actuation are different from device to device due predominantly to differences in the grown device geometries. Although the catalyst areas are identical in each case, small fluctuations in the growth conditions can lead to different final structure geometries. For all devices studied here, the walls were bent outwards after growth, giving a larger separation at the top than the nominal 10 μm at the bottom of the walls. This is clearly seen in Fig. 1(b) and Figs 2 (e)-(h). It should be possible to adjust the growth conditions to avoid this problem in future.

It is possible to reproducibly vary the separation of the top of the nanotube walls for many cycles as long as the applied voltage stays below the pull-in voltage (this is the voltage beyond which the structures make physical contact). An example of multiple actuation cycles is shown in Fig. 3 (for this particular device, the nanotube walls had a thickness of 6 μm). When the pull-in voltage is exceeded the nanotubes make contact and the high current that can then flow between the walls leads to destruction of the nanotubes. As expected for MEMS switches and discussed in detail for carbon nanotube devices, the distance at which pull-in occurs is at approximately 67% of the initial gap spacing [13]. It is interesting that although the carbon nanotube walls are extremely porous, with only 10^{10} nanotubes cm^{-2} corresponding to a porosity of > 95%, they move as a single cohesive unit.

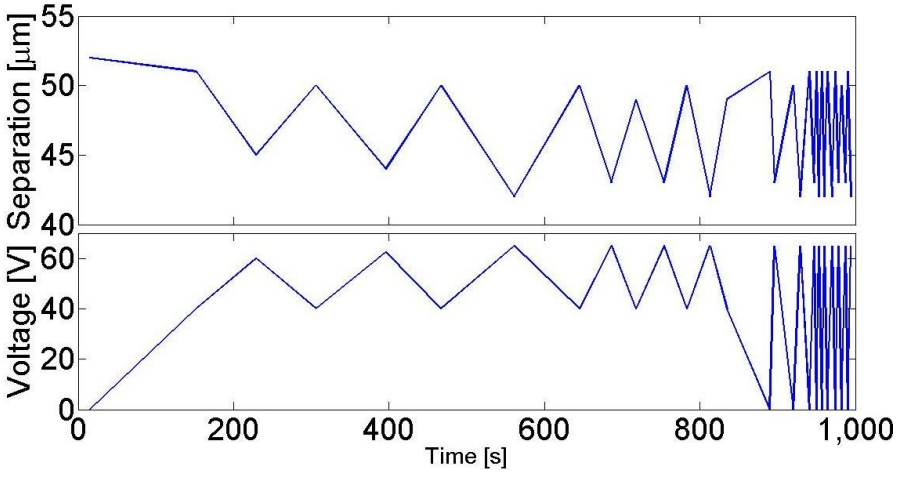

Figure 3. Correlation between the voltage applied between the CNT walls and the separation at the top of the walls. The voltage was varied between 0 V and a voltage just below the pull-in voltage for the device.

Simulation results obtained for devices with the same density, height (135 μm) and width (4 μm) of the nanotube walls and having a higher separation at the top (60 μm) than at the base (10 μm), in good agreement with experimental geometries, are shown in Figure 4. Figure 4(a) shows the main deformation regions predicted by the model under actuation. Figure 4(b) shows the simulated deflections as a function of applied voltage for four different values of Young's modulus. The simulations also show that pull-in occurs for a separation of ca. 67% of the initial gap. In order to achieve actuation for voltages of a few tens of volts, as seen in the experiments, the effective Young's modulus, E, of the nanotube films has to be very low. Individual multi-walled nanotubes have values of E that range from ca. 800 GPa for high quality arc-discharge grown nanotubes to 10-50 GPa for defect-rich catalytically grown samples [14]. We can expect that our individual CVD grown MWNT typically have values between these two extremes. The displacement at the top of the nanotube arrays for a given applied voltage scales with $1 / \sqrt{(EI)}$ [15] so, if the CNT walls had a Young's modulus equivalent to that of individual multiwalled nanotubes, the pull-in voltage for capacitor walls of the dimensions used in the present work would lie in the range 3.9 kV - 35 kV. The CNT walls are low density structures with "curly" nanotubes, shown in Fig. 5(a),(b), making it rather easy for the nanotubes to slip and slide against each other, thus forming a material with a very low effective Young's modulus.

In order to compare the simulation results with the experiments, we consider the change in the wall separation as a function of applied voltage. Figure 5 (c) shows the results for the device shown in Fig. 2(a). The full line is the simulated behaviour for a Young's modulus of 3.8 MPa. The value of E obtained from the comparison between experiments and simulations is much lower than the value estimated for devices fabricated out of densified nanotube films (ca. 10 GPa) [16]. These films have been treated to have a much higher density (42%) than the directly grown films studied here. The best nanotube yarns (formed by spinning carbon nanotubes) have values on the order of 150 – 460 MPa [17]. The most direct comparison is with the properties of compressive films of multiwalled nanotubes, grown in a similar fashion to our samples [18] that have been shown to have elastic moduli on the order of 6 MPa due to the ease of bending of the individual nanotubes in the films.

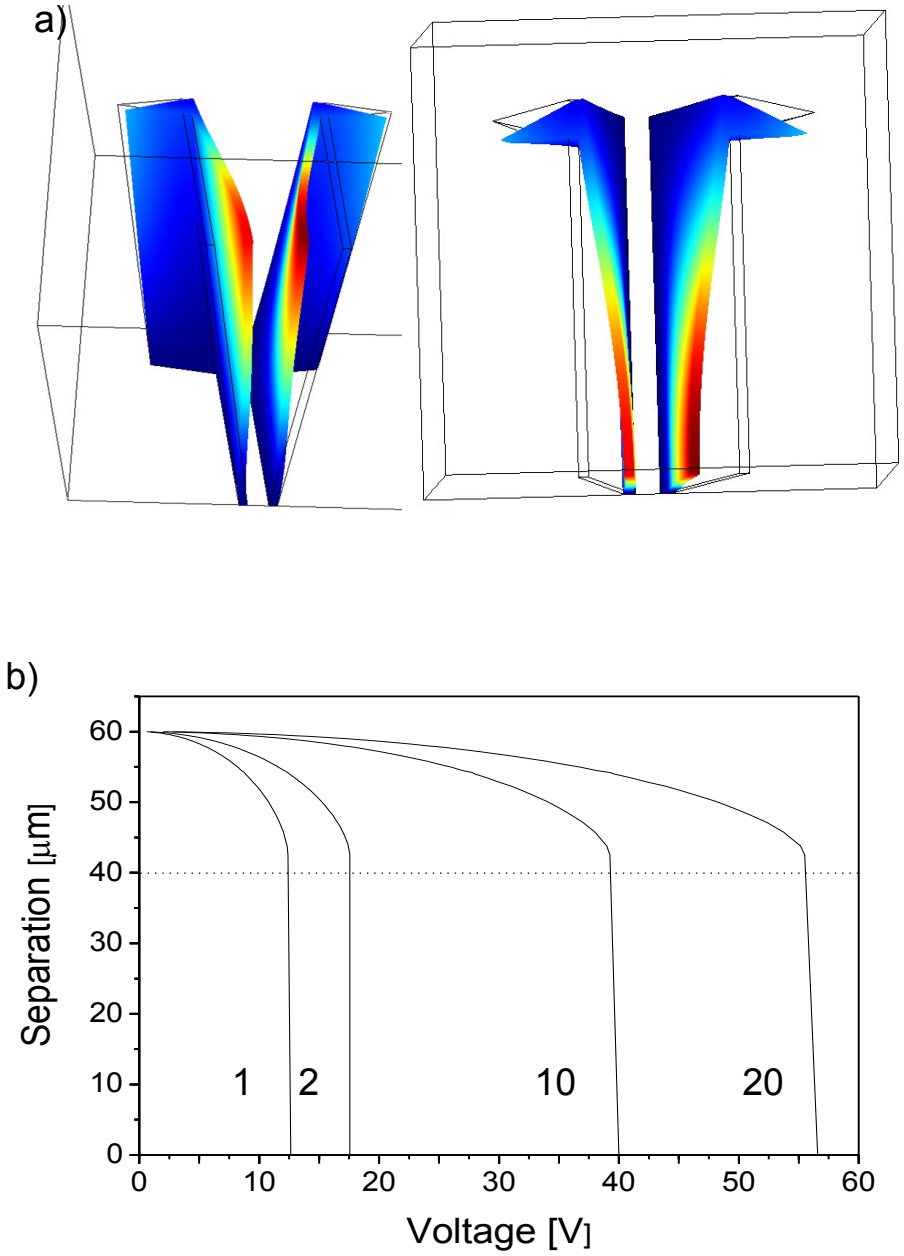

Figure 4. (a) model of electrostatic actuation of nanotube walls for a voltage just at pull-in. Left: side view, Right: top view. The colours indicate the amount of deflection (0 µm for dark blue to 8.3 µm for dark red). (b) Simulations of the separation at the top of the nanotube walls (assuming an initial gap of 60 µm, with a base gap of 10 µm) for four different values of Young's modulus: 1 MPa, 2 MPa, 10 MPa and 20 MPa (corresponding numbers shown onplot). The pull-in voltage scales with the square root of the Young's modulus as expected (28 V, 39 V, 55 V and 175 V). The dashed line indicates a separation of 67% of the initial gap, indicating the separation for which pull-in is expected to occur.

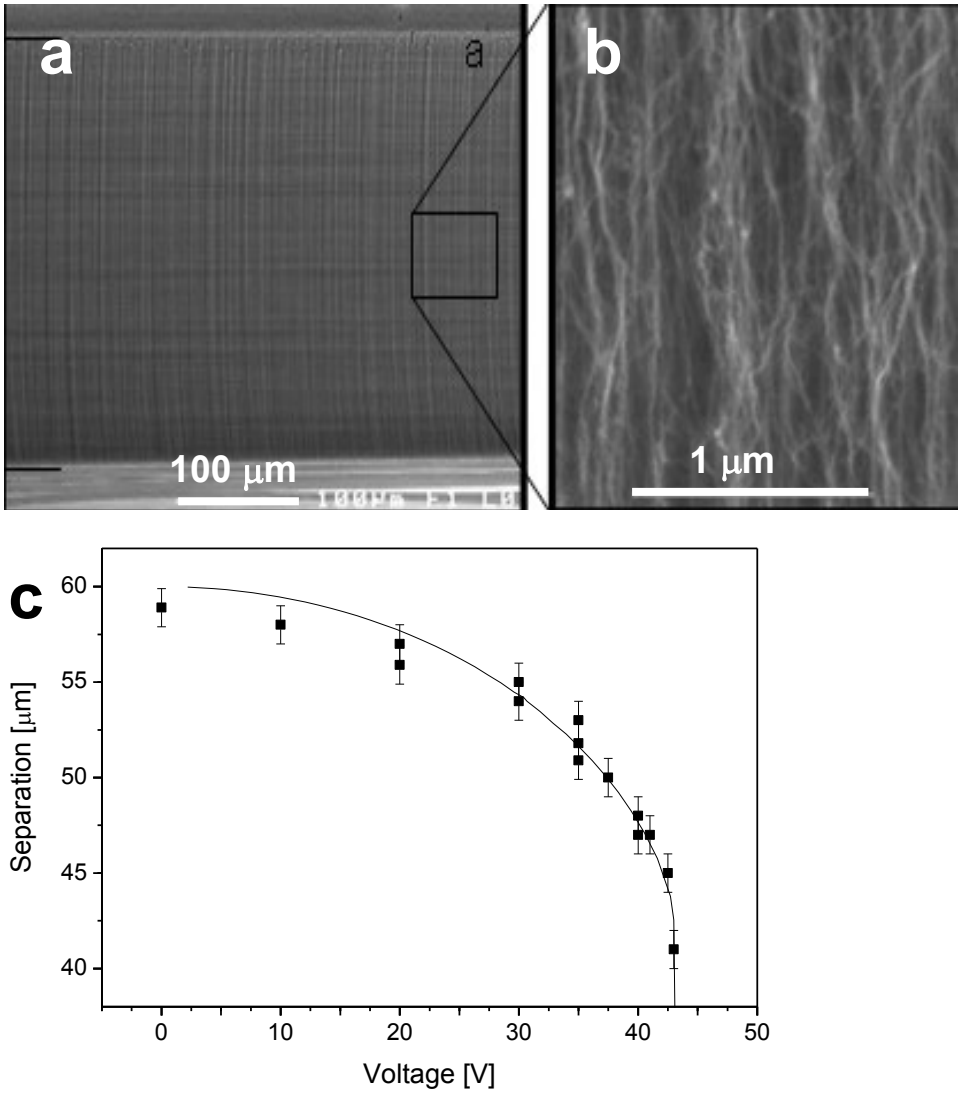

Figure 5. (a),(b) SEM pictures of a typical nanotube array showing the sparse and "wiggly" nature of the quasi-aligned nanotubes. (c) Measured separation at the top of the nanotube walls versus applied voltage for the varactor device of Fig. 2(a). The full line gives the results of the COVERTOR simulations using a Young's modulus of 3.8 MPa.

4. Determination of Capacitance

The capacitance of the devices was determined by measuring the S-parameters in the frequency range from 200 MHz to 1.5 GHz. The values were extracted from experimental measurements by considering the equivalent electrical circuit model shown in Fig. 6(a). Results are shown in Fig. 6(b) for an actuation voltage of 0 V and 27.5 V, for the device shown in Fig. 1(b) along with the results of fitting the equivalent circuit model. The capacitance values inherent to the geometry of the substrate layout were found from calibration measurements on OPEN samples without any nanotubes ($C_{Ground1} = C_{Ground2} = 110$ fF and $C_{parasitic} = 5.8$ fF).

The insertion losses of the conductor wires were measured on THRU samples and were found to be 14 dB. These losses were modelled by the two resistances R1 = R2 = 190 Ω. The static capacitance between the nanotube walls was found experimentally to be 22 fF. This can be compared with the results of the HFSS simulations that yielded 5.6 fF for the parasitic capacitance of the electrode pattern and 27 fF for the electrode plus nanotube structure. The electrostatic formula for a parallel plate capacitor $C = \varepsilon_0 A / d$ gives a value of 23.9 fF where ε_0 is the vacuum electrical permittivity, A is the area between the plates and d is the separation between them.

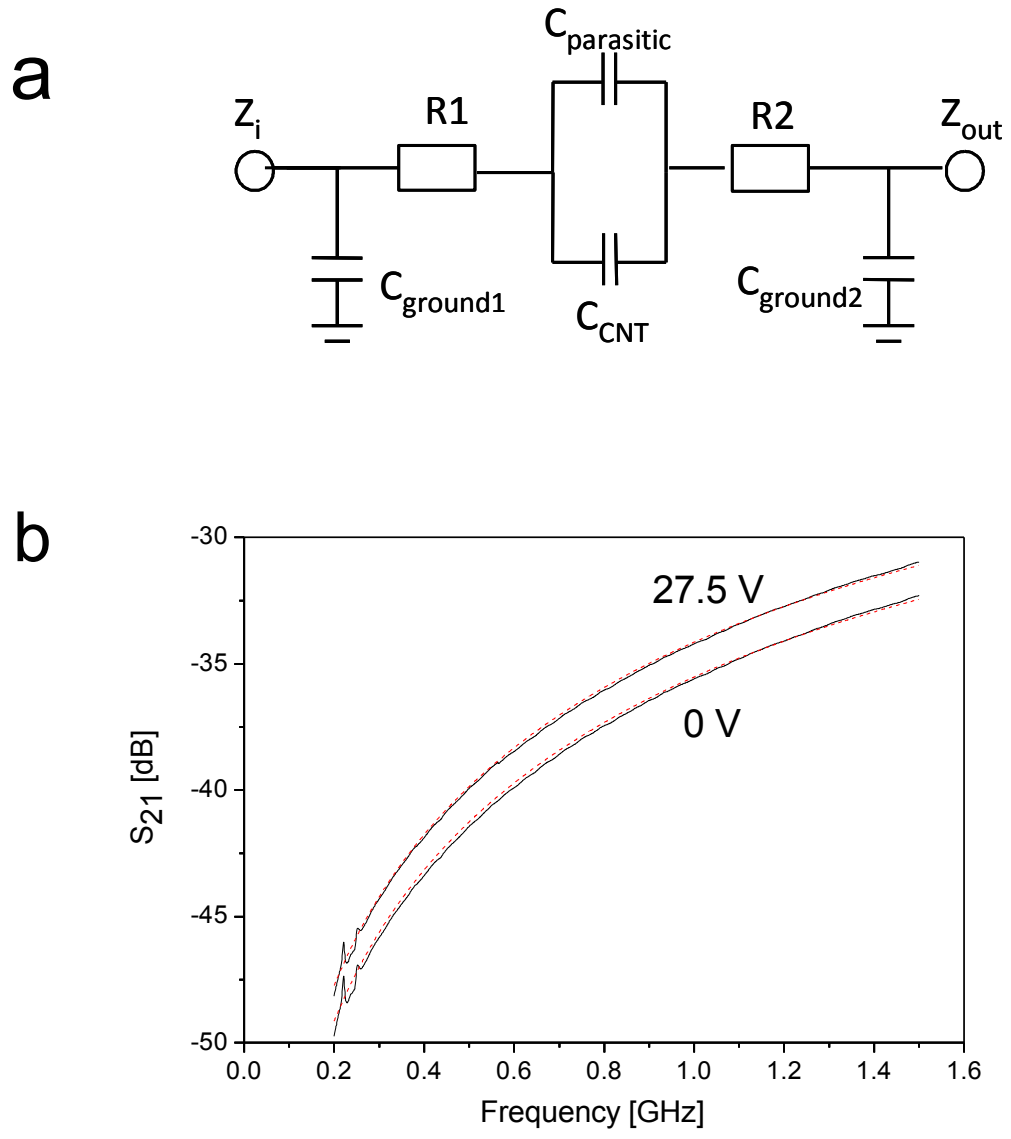

Figure 6. (a) Equivalent circuit used to fit the experimental results. (b) S_{21} parameter measured for the frequency range 200 MHz – 1.5 GHz for 0 V and 27.5 V actuation voltage, close to the pull-in voltage for this device (full, black line). The equivalent circuit model fits are also shown (red dashed lines).

The capacitance change as a function of the actuation voltage is plotted in Figure 7(a). The capacitance was increased to 27 fF when applying a voltage of 27.5 V, shortly before the pull- in voltage was reached. This corresponds to a change in capacitance of over 20%. The capacitance could be reproducibly varied up to the value of the pull-in voltage. When the actuation voltage was increased beyond the pull-in voltage the nanotube walls made contact, leading to a sharp decrease in the value of the capacitance, after which reproducible behaviour could again be observed but with a shift downwards in the absolute capacitance of the device. The SEM pictures in Figs. 7(b) and (c) show the device after measurement. The nanotubes have obviously made contact in the upper central part of the device (the part that experiences the maximum deflection). The high current that flowed on contact has removed the nanotubes from one side of the structure leaving a large hole, however, the device can still operate as a varactor with an overall decrease of the capacitance for a given actuation voltage. The *Q*-factor can be extracted from the measurements using the simple formula $Q = \frac{1}{2\pi fRC}$, where f is the frequency, R the resistance and C the capacitance of the device. The results are plotted in Fig. 8 for both the non-actuated (0 V) and actuated (27.5 V) devices in the frequency range 0.2 – 1.5 GHz. The *Q*-factor ranges from 100 to 10 as the frequency increases. The losses are dominated by the relatively poor conductance of the sputtered Mo electrodes.

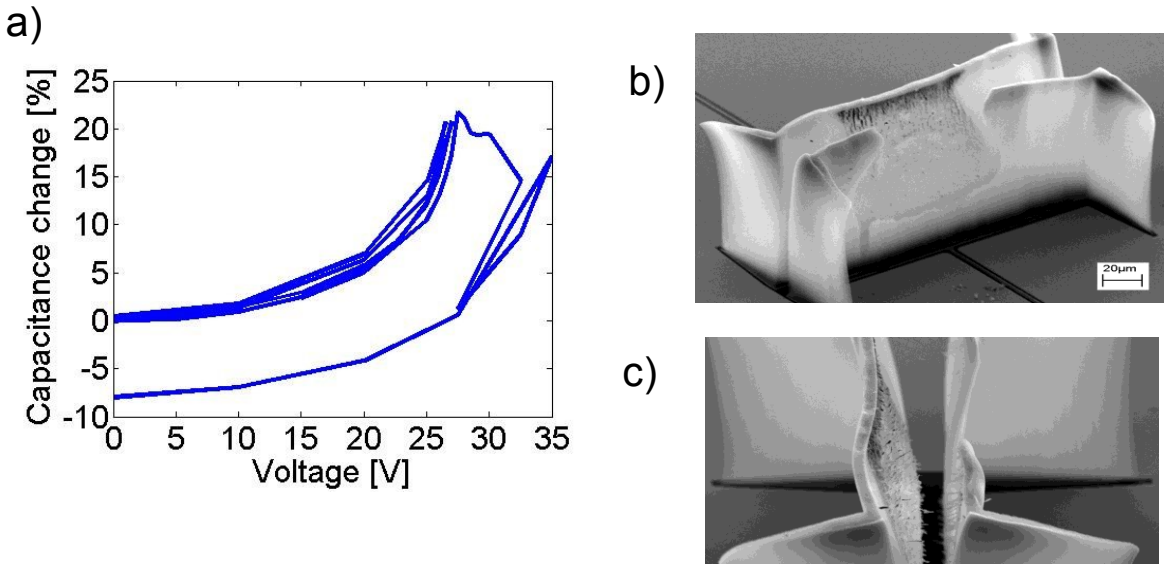

Figure 7. (a) Capacitance change versus actuation voltage (b), (c) SEM pictures of device after measurement.

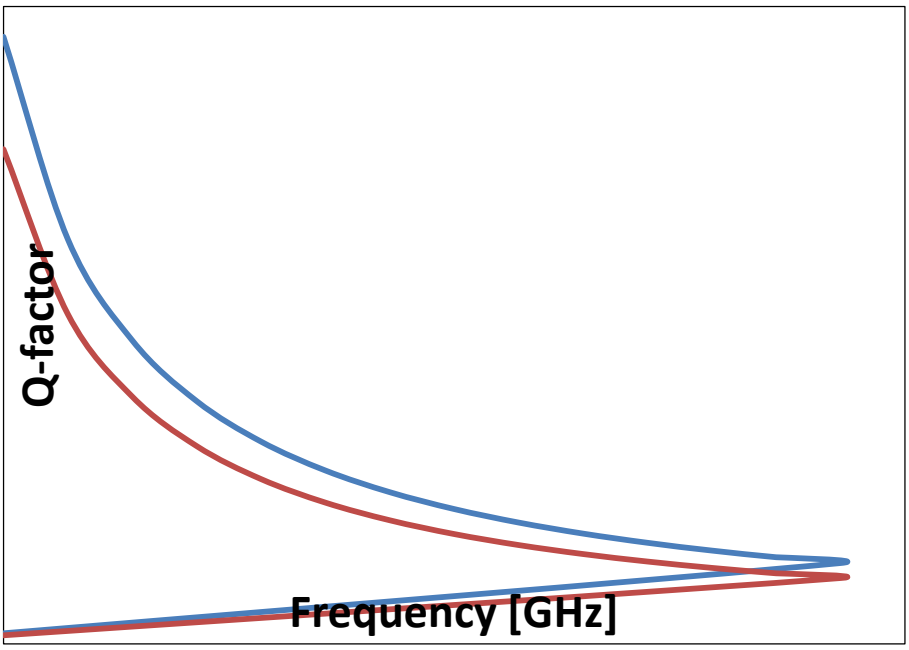

Figure 8. *Q*-factor extracted from the measured resistance and capacitance as a function of RF frequency. Upper (blue) line: non-actuated device (0 V), Lower (red) line: actuated device with an applied voltage of 27.5 V between the nanotube walls.

5. Conclusions

We have fabricated a varactor based on two parallel plates formed from arrays of multiwalled carbon nanotubes. A comparison between the experimentally determined actuation and model calculations allowed an estimate of the effective Young's modulus of the nanotube films. The very low value (ca. 4 MPa) compared to the Young's modulus of individual carbon nanotubes allows relatively large structures to be actuated with rather low voltages. The capacitance was determined from RF transmission measurements and a capacitance change of over 20% was found. This is presently limited due to the geometry of the device and the fact that the bases of the nanotube walls are fixed on the substrate. However, the good agreement between model calculations and the experimental measurements now makes it possible to design device geometries for specific operating characteristics. The low mass and resistance to conditions of high temperature make devices based on carbon nanotubes interesting for a range of applications. This work shows that arrays of vertically aligned carbon nanotubes behave as extremely low density conductive bulk material and can be used as building blocks for MEMS and NEMS devices. We have also demonstrated *in situ* nanotube growth on a substrate and layout that still permits ultra-sensitive direct RF detection after exposure to standard nanotube growth conditions.

References

[1] e.g. Meyyappan, M. 2005 Carbon Nanotubes Science and Applications (Boca Raton, FL: CRC Press)

[2] Xu, T., Wang, Z., Miao, J., Chen, X., Tam, C.M., 2007 Appl. Phys. Lett. **91** 042108.

[3] Fan, S., Chapline, M.G., Franklin, N.R., Tombler, T.W., Cassell, A.M., Dai, H., 1999 Science **283** 512.

[4] McCarter, C.M., Richards, R.F., Mesarovic, S. Dj., Richards, C.D., Bahr, D.F., McClain, D., Jiao, J. 2006 J. Mater. Sci. **41** 7872.

[5] Aliev, A.E., Oh, J., Kozlov, M.E., Kuznetsov, A.A., Fang, S., Fonseca, A.F., Ovalle, R., Lima, M.D., Haque, M.H., Gartstein, Y.N., Zhang, M., Zakhidov, A.A., Baughman, R.H., 2009 Science **323** 1575.

[6] Puretsky, A.A., Geohegan, D.B., Jesse, S., Ivanov, I.N., Eres, G. 2005 Appl. Phys. A. 81 223.

[7] Cao, A., Dickrell, P.L., Sawyer, W.G., Ghasemi-Nejhad, M.N., Ajayan, P.M., 2005 Science **310** 1307.

[8] Jeong, G.H., Olofsson, N., Falk, L.K.L., Campbell, E.E.B., 2009 Carbon **47** 696.

[9] Rong, B., Burghartz, J.N., Nanver, L.K., Rejaei, B., van der Zwan, M. 2004 Electron Device Letters IEEE **25** 176.

[10] Eriksson, A., Lee, S.W., Sourab, A.A., Isacsson, A., Kaunisto, R., Kinaret, J.M., Campbell, E.E.B. 2008 Nano Lett. **8** 1224.

[11] Ek-Weis, J., Eriksson, A., Idda, T., Olofsson, N., Campbell, E.E.B. 2009 J. Nanoeng. and Nanosystems in press

[12] Vijayaraghavan, A., Blatt, S., Marquardt, C., Dehm, S., Wahi, R., Hennrich, F., Krupke, R., 2008 Nano Res.**1** 321.

[13] Desquesnes, M., Rotkin, S.V., Aluru, N.R. 2002 Nanotechnology **13** 120.

[14] Salvetat J.P.,Kulik, A.J., Bonard, J.M., Briggs, G.A.D., Stockli, T., Metenier, K., Bonamy, S., Beguin, F., Burnham, N.A., Forro, L. 1999 Adv. Mater. **11** 162.

[15] Landau, L.D., Lifschitz, E.M., 1981 Theory of Elasticity (Ed. 2, Pergamon Press)

[16] Hayamizu, Y., Yamada, T., Mizuno, K., Davis, R.C., Futaba, D.N., Yumura, M., Hata, K. 2008 Nature Nanotechn. **3** 289.

[17] Zhang, M., Atkinson, K.R., Baughman, R.H. 2004 Science **306** 1358.

[18] Cao, A., Dickrell P.L., Sawyer, W.G., Ghasemi-Nejhad, M.N., Ajayan, P.M., 2005 Science **310** 1307.